Detection and characterization of changes of the correlation structure in multivariate time series

Markus Müller* and Gerold Baier
Facultad de Ciencias, Universidad Autónoma del Estado de Morelos, 62210 Cuernavaca, Morelos, Mexico

Andreas Galka
Institut für Experimentelle und Angewandte Physik, Christian-Albrechts-Universität, 24098 Kiel, Germany and Institute of Statistical Mathematics (ISM), Minami-Azabu 4-6-7, Minato-ku, Tokyo 106-8569, Japan

Ulrich Stephani and Hiltrud Muhle
Klinik für Neuropädiatrie, Christian-Albrechts-Universität, 24105 Kiel, Germany
(Received 9 June 2004; published 14 April 2005)

We propose a method based on the equal-time correlation matrix as a sensitive detector for phase-shape correlations in multivariate data sets. The key point of the method is that changes of the degree of synchronization between time series provoke level repulsions between eigenstates at both edges of the spectrum of the correlation matrix. Consequently, detailed information about the correlation structure of the multivariate data set is imprinted into the dynamics of the eigenvalues and into the structure of the corresponding eigenvectors. The performance of the technique is demonstrated by application to N_f-tori, autoregressive models, and coupled chaotic systems. The high sensitivity, the comparatively small computational effort, and the excellent time resolution of the method recommend it for application to the analysis of complex, spatially extended, nonstationary systems.

DOI: 10.1103/PhysRevE.71.046116 PACS number(s): 02.50.Sk, 05.45.Tp, 89.75.−k, 05.10.−a

I. INTRODUCTION

For spatially extended dynamical systems it is typical that numerous constituents are involved in the procreation of various possibly independent transient processes, which might occur simultaneously, such that the dynamics of the system is characterized by a complex spatiotemporal correlation pattern. An important example is electric brain activity as measured by conventional electroencephalographic recordings where information processing is realized by an ever-changing degree of synchronization between neural assemblies [1]. This complicated dynamics, characterized by the permanently changing extent of collectivity of the system (or of dynamically formed subsystems), is reflected in the continuously varying degree of synchronization between subsets of the corresponding time series within multivariate data sets. Hence, suitable tools for the detection and quantitative description of such situations are needed.

Among the established tools of time series analysis many have been designed predominantly for the scalar case (e.g., Fourier based techniques [2], wavelet analysis [3], or time-delay embedding [4]), and even in cases where this limitation is not strictly imposed, there is still a widespread tendency to condense the complexity of the system into just one single descriptive parameter, such as the correlation dimension [5]. Another example, which recently has attracted considerable attention, is phase synchronization in coupled dynamical systems [6]. The power spectrum itself is not suitable for the detection of phase synchronization; therefore the Hilbert transform [7] is usually employed for this purpose. However, in the case of time series with a broad power spectrum the extracted intantaneous phases have no physical meaning [6]. A method particularly designed for the analysis of multivariate time series is independent component analysis [8]. This approach provides a decomposition of data into independent source signals, and in situations where the assumption of independence is appropriate, it is a suitable method [9].

Recently techniques known from random matrix theory (RMT) have been applied to the analysis of the equal-time correlation matrix **C** constructed from empirically obtained multivariate data sets [10–19]. This approach offers the possibility to compare the fluctuation properties of the spectrum of **C** with the analytical results obtained for random matrix ensembles [20]. It is assumed that the part of the spectrum which can be described by random matrices should be governed by random correlations or noise; only those eigenvalues (and corresponding eigenvectors) which show significant deviations from the RMT predictions, contain genuine information about the "true" correlation structure of the system. It was found that in particular the upper part of the spectrum of **C** lies far outside the analytical RMT results. Consequently, the authors concluded that the entire rest of the spectrum does not reflect any relevant information [10,12,13,15,16,19].

In this paper we present an approach for the analysis of multivariate data sets based on the temporal evolution of eigenvalues and eigenvectors of **C**. The main objectives of the present study are as follows.

(1) We present a conceptually simple and yet powerful framework for detecting and characterizing time dependent phase-shape correlations.

(2) Inspired by previous work in the field of open quantum systems [24,25], we explain the mechanism by which

*Email address: muellerm@servm.fc.uaem.mx

information about the correlation structure of multivariate time series is induced in the spectrum of **C**.

(3) We show that in general the lower part of the spectrum of eigenvalues and eigenvectors is *not* dominated by noise and/or random correlations, but also contains essential information about the correlation dynamics of the system. We present evidence supporting the concept that there exist situations for which the lower part of the spectrum contains statistically more relevant information than the largest eigenvalues and their corresponding eigenvectors.

(4) We show how the analysis of the largest and smallest eigenvalues and their corresponding eigenvectors can be combined to extract details of changes in the correlation pattern.

The paper is organized as follows. After discussing the method itself and the relevant quantities in the next section, we demonstrate its performance by applying it to three classes of artificially generated multivariate time series in Secs. III, IV, and V. In particular we show results for the analysis of systems given by sums of sine waves with incommensurable frequencies, for stochastic oscillations generated by linear multivariate autoregressive models, and for coupled chaotic systems. In Sec. VI we present a comparison with other approaches. While most results presented in this paper have been obtained from artificially generated time series, in Sec. VII we briefly also discuss an application to a clinical electroencephalogram (EEG); we expect that EEG recordings may form an important field of application for the method to be discussed in this paper. In Sec. VIII we examine the relation between the results obtained by the application of random matrix theory to correlation matrices and those obtained in this paper.

II. BASIC METHODOLOGY

In order to analyze two-point correlations in multivariate time series with unknown stationarity properties we evaluate the correlation matrix over a moving window of length Δt containing N data points where each data point $X_i(t_k)$ is normalized according to

$$\tilde{X}_i(t_k) = \frac{X_i(t_k) - \overline{X_i}}{\sigma_i}, \tag{1}$$

where $\overline{X_i}$ and σ_i denote the mean value and standard deviation, respectively, of the original time series $X_i(t_k)$ within the window Δt, and k labels all data points within the window. Individual time series $X_i(t_k)$ of the multivariate data set are labeled by i, where $i=1,\ldots,M$. Based on this time window, which is shifted over a given set of time series with the maximally possible overlap of $N-1$ data points, the equal-time correlation matrix **C** is computed by [21,22]

$$C_{ij}(t_l) = \frac{1}{N}\sum_k \tilde{X}_i(t_k)\tilde{X}_j(t_k), \tag{2}$$

where t_l is the center value of the current time window Δt. Provided the window size Δt is chosen sufficiently small, the normalization Eq. (1) has the effect of removing amplitude information from each time series within the window, such that the measured cross correlations reflect exclusively relationships between the shapes and phases of the signals. Furthermore, the normalization provides a well defined scale, such that the matrix elements of **C** vary between +1 (completely correlated state) and −1 (completely anticorrelated state). For the particular case of sinusoidal signals these states correspond to the interval of possible phase differences between two signals. A special case is given for a phase difference of $\pi/2$, which according to this definition leads to zero correlation; we shall call this a *noncorrelated* state.

The window size Δt defines the time scale on which the correlations are measured. If the window size is increased, statistical fluctuations of the calculated quantities will decrease, but at the same time the temporal resolution of the results will also decrease. Hence, in any practical application one has to find a compromise between averaging out the noise components via the sum in Eq. (2) and the required time resolution. For all cases presented in this paper we checked various sizes of Δt, obtaining qualitatively the same results. If not mentioned explicitly, we fix the window size to $N=2048$ sampling points throughout this paper; defining an arbitrary time unit of 256 sampling points length, this window size corresponds to $\Delta t=8$ time units.

As a central concept we employ the eigenvalues λ_i and eigenvectors $\vec{v}_i$ of the correlation matrix **C**: $\mathbf{C}\vec{v}_i=\lambda_i\vec{v}_i$; the eigenvalues λ_i will be ordered according to size, such that $\lambda_1 \leqslant \lambda_2 \leqslant \cdots \leqslant \lambda_M$. The distribution of the eigenvalues is directly related to the amount of correlations of the multivariate data set. This can be easily understood by considering some general properties of the equal-time correlation matrix, Eq. (2).

(i) Each diagonal element of **C** is equal to 1, because each time series $X_i(t)$ is perfectly correlated with itself. Hence, the sum of the eigenvalues is time independent and equal to M, the dimension of the multivariate data set. As a consequence, the change of any of the eigenvalues has to be compensated by a corresponding change of at least one of the others.

(ii) For noncorrelated $X_i(t)$ the values of the nondiagonal elements of **C** tend to zero if the time window Δt tends to infinity ($\lim_{\Delta t\to\infty} C_{ij}=0 \ \forall \ i\neq j$). In that case the spectrum of **C** is completely degenerate and $\lambda_i=1 \ \forall \ i$. For any finite value of Δt, however, the values of C_{ij}, $i\neq j$, remain finite, which leads to a lifting of the degeneracy. In this case the eigenvalues are distributed around 1, reflecting the presence of random correlations within the finite window Δt.

(iii) In the case when all M time series are perfectly correlated (i.e., they are identical), $C_{ij}=1 \ \forall \ i,j$. This matrix has only one nonzero eigenvalue, $\lambda_{20}=M$.

These extremes (for noncorrelated and perfectly correlated time series) allow a quantitative description of the correlation pattern of a given data set. For the time dependent case of nonstationary time series the evaluation of the correlation matrix over a moving window with finite Δt is required [Eqs. (1) and (2)].

When analyzing recordings from spatially extended complex systems it is desirable to measure how strongly and in what manner the different components of the systems cooperate, i.e., to detect and characterize collective dynamics. The classification of collective phenomena in complex sys-

tems is well elaborated in many fields of physics, in particular in many-body theory. As an example we mention the interpretation of giant resonances as the collective motion of nucleons [23]. These collective modes involving many particles are interpreted as constructive interferences of numerous single-particle states causing a large spreading width [23,26]. Hence, the resulting multiparticle eigenstate describing the collective dynamics of the nucleus contains considerable contributions from each of the single-particle states involved. On the other hand it is known that the collectivity of a particular eigenstate increases via level repulsions with other eigenstates [24–26]. Two repelling states interfere such that the resulting eigenvectors are a symmetric and an antisymmetric mixture of the original states. By this mechanism a separation of one or several eigenvalues occurs resulting in well pronounced collective properties of the corresponding eigenstates involved [24,25].

The degree of collectivity of such states with respect to a well defined basis can be quantified by the participation ratio or the *number of principal components*. Let a_{ij} denote the expansion coefficients of eigenvector $\vec{v}_i$; then the number of principal components is defined as [14,25]

$$N_i^p = \frac{1}{M\sum_j |a_{ij}|^4}. \tag{3}$$

This quantity measures the percentage of basis states needed to construct the eigenstate $\vec{v}_i$. If the a_{ij} are uniformly distributed (all basis states j contribute equally to the expansion of eigenstate i) N_j^p is equal to 1. If $\vec{v}_i$ contains only a few components N_j^p takes values close to $1/M$, where M is the dimension of the configuration space.

Because each row (or, equivalently, each column) of **C** represents the two-point correlations between a particular signal $\tilde{X}_i(t)$ and all others, each basis vector represents the cross correlations measured in one time series or data channel i. For this reason we might call this basis the "channel basis." Hence, the number of principal components N_i^p reflects the amount of cross correlations contributing to the ith eigenstate, and in this sense it is a measure of the degree of collectivity. Intuitively one might understand collectivity as the cooperative behavior of many components of a system, as for example when they synchronize their dynamics. We will see that the abstract concept of the number of principal components exactly fits this intuitive picture.

The definition of N_i^p does not permit one to discriminate between correlation and anticorrelation. Therefore a second quantity is needed which takes into account the sign of the a_{ij} and hence the approximate orientation of the eigenvector in the configuration space. We call it the *symmetry parameter* and introduce a definition such that it becomes unity for completely symmetrical and zero for completely antisymmetrical states:

$$S_i = \left| \sum_j \mathrm{sgn}(a_{ij}) |a_{ij}|^2 \right|. \tag{4}$$

This quantity enables us to measure to what extent an eigenvector is generated by constructive or destructive interference of basis states.

III. MULTIVARIATE N_F-TORI

To demonstrate the performance of the method we consider a standard class of dynamical systems, a sum of N_f sine waves with mutually incommensurate frequencies. Time series of such systems sample N_f-tori [27], i.e., geometrical objects with topological dimension equal to N_f. Because of the flexibility of this system class and the fact that its dynamics and hence the correlation structure can be perfectly controlled, it serves as an ideal test system for the method discussed in this paper.

A. Definition and design of the system

N_f-tori are generated by sums of N_f harmonic oscillations; here we choose equal amplitudes for all oscillations:

$$X_i(t) = \sum_{j=1}^{N_f} \sin(2\pi f_j t + \delta_{ij}), \quad i = 1, \ldots, M, \tag{5}$$

where the set of frequencies f_j is sampled randomly from a uniform distribution on the interval $[0, f_{\max}]$ with $f_{\max}=20$ frequency units. In this paper one time unit is arbitrarily defined as 256 data points. The same set of frequencies is chosen for all i, whereas the set of random partial phases δ_{ij} is assigned from the interval $[0, 2\pi]$ to each time series i independently. In all examples of N_f-tori we have chosen $N_f=1000$ frequencies and $M=20$ time series.

The correlation structure of this multivariate data set is controlled by the partial phases δ_{ij}. If the δ_{ij} are uniformly distributed between zero and 2π the $X_i(t)$ are mutually uncorrelated. Any deviation from the uniform distribution will result in phase-shape correlations between the time series. We generate phase-shape correlations via Gaussian distributions modulo 2π with prespecified mean μ_δ and variance σ_δ^2.

In general, phase correlations may affect all frequencies, or they may be limited to a certain frequency band, while oscillations outside of this band retain uncorrelated partial phases. In order to simulate such a situation we can choose the δ_{ij} as Gaussian distributed only for a subset of the N_f frequencies corresponding to a certain frequency band.

Nonstationary time series with time dependent correlation structure will now be generated in the following manner. The time series are composed of three consecutive segments, each of 5120 sampling points length (corresponding to 20 time units). For the first segment a set of partial phases δ_{ij} is randomly chosen from a uniform distribution independently for each channel i and kept constant during this period. Then a new set of random partial phases δ'_{ij} is chosen from a Gaussian distribution (modulo 2π) with a given mean μ_δ and variance σ_δ^2. These partial phases are arbitrarily assigned to the oscillations f_j of each channel i. Then, during the second segment each of the uniformly distributed partial phases δ_{ij} is linearly shifted toward the corresponding new set of δ'_{ij}. This step may be limited to those oscillations belonging to a certain frequency band or to partial phases belonging to a certain subset of channels. Finally, at the end of the second time segment, the partial phases have reached their Gaussian-distributed values. During the third time segment all partial phases are kept constant.

TABLE I. Listing of different N_f-tori analyzed in this paper.

System	Characteristics of the transition in second time series segment
A	For all channels the partial phases of the 25% lowest frequencies are shifted linearly to a Gaussian distribution with $\sigma_\delta=\pi/2$ and $\mu_\delta=\pi/2$, the remaining partial phases remaining uniformly distributed values
B	As in system *A*, but here the partial phases of 50% of the lowest frequencies are shifted
C	As in system *A* but here the partial phases of 100% of the lowest frequencies are shifted
D	All partial phases of two channels are shifted linearly to a Gaussian distribution with $\sigma_\delta=\pi/4$ and $\mu_\delta=\pi/2$, the partial phases of all other channels remaining uniformly distributed values
E	All partial phases of four channels are shifted linearly to a Gaussian distribution with $\sigma_\delta=\pi/12$; the four channels are divided in two groups of two channels each, such that between the means μ_δ of these groups a phase difference $\Delta\delta=\pi$ exists; the partial phases of the remaining channels remain uniformly distributed values
F	As system *E*, but with $\Delta\delta=\pi/2$

Hence, the resulting data set is stationary during the first and last segments, i.e., between time units 0 and 20, and between time units 40 and 60. From time units 20 to 40 (the central segment) a linear transition between the two dynamical stationary "states" takes place. A set of different systems is defined by different choices of the properties of this transition occurring during the central segment. Table I lists the systems that will be employed as exemplary testing systems in this section.

B. Correlations extending over all time series

First we will focus on the analysis of systems *A*, *B*, and *C*, where phase correlations are induced simultaneously in all $M=20$ time series. In Fig. 1(a) we compare the temporal evolution of the largest eigenvalue λ_{20} for system *A* (dotted line), system *B* (dashed line), and system *C* (solid line). It can be seen that for all three systems λ_{20} keeps a small average value slightly above 1 during the first 20 time units, i.e., the noncorrelated segment. Slight deviations from unity during this segment are caused by random correlations which influence the analysis for any finite size of Δt. Between 20 and 25 time units λ_{20} increases abruptly. For the cases of systems *B* and *C* λ_{20} encounters a local maximum at ca. 30 time units, and in the last segment it fluctuates around a value of 5 for system *C*, around 3 for system *B*, and slightly above 2 in the case of system *A*. The relative change of λ_{20} from the first to the third segment is on the average 230% for system *C*, 100% for system *B*, and still 47% for system *A*. λ_{20} starts to increase almost immediately after the partial phases have started to shift from their uniformly distributed initial values to the Gaussian-distributed final values. At the same time as λ_{20} increases, all other eigenvalues λ_i, $i=1,\ldots,19$, decrease (not shown in the figure). Furthermore, it is remarkable that the tiny changes of the phase distribution in the case of system *A* are clearly visible in the changes of λ_{20}. This behavior can be qualitatively understood by the general arguments (i)–(iii) discussed in the previous section. The deformation of the phase distribution toward a Gaussian causes an increase of the degree of synchronization between all *M* time series. Hence, the largest eigenvalue tends to separate from the rest and assumes larger values, as described by (iii). It can be concluded that the system performs a global transition to a more synchronized dynamics, if simultaneously all smaller λ_i decrease.

So far the local maximum of λ_{20} between time units 30 and 40, which is visible at least for the cases of systems *B* and *C*, has not been explained. Since the order of the partial phases within the interval $[0,2\pi]$ is not maintained during the transition from the uniform to the Gaussian distribution during the second time segment, there occur numerous crossings between pairs of δ_{ij} during this segment. Consequently the distribution of partial phases will transiently become nar-

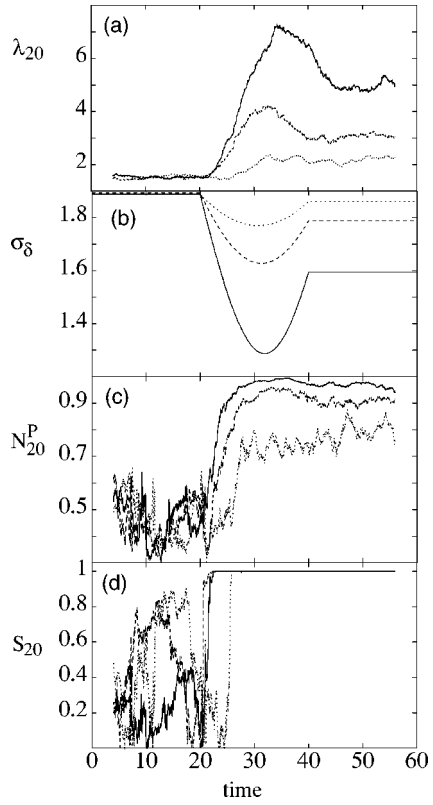

FIG. 1. Time evolution of (a) the largest eigenvalue λ_{20}, (b) the standard deviation of the phase distribution σ_δ, (c) number of principal components N_{20}^p, and (d) the symmetry parameter S_{20} of the largest eigenvector $\vec{v}_{20}$. The figure displays the results for systems *A* (dotted line), *B* (dashed line), and *C* (solid line) of Table I. The time scale is given in arbitrary units as explained in the text.

rower than the final Gaussian distribution, whence a minimum of the width of the phase distribution is caused. This phenomenon is visualized in Fig. 1(b), where the standard deviation of the phase distribution is shown for systems *A*, *B*, and *C* as a function of time. If, as in the case of systems *B* and *C*, the minimum of the phase distribution is sufficiently pronounced, it is reflected by a local maximum of λ_{20}. This example demonstrates that changes of the correlation structure of these multivariate time series cause changes in the dynamics of the eigenvalue spectrum of the correlation matrix.

In the present case, where all time series are being correlated simultaneously, a repulsion between the largest eigenvalue and the entire rest of the spectrum is observed. It is well known that level repulsions cause a mixing of the eigenstates with well defined symmetry properties [24,25]. Therefore, the observed transition should also be reflected in the properties of the eigenvectors. Figures 1(c) and 1(d) show the results for the number of principal components N_{20}^p and the symmetry parameter S_{20} of the eigenvector corresponding to the largest eigenvalue for the case of systems *A*, *B*, and *C*. Both quantities N_{20}^p and S_{20} show a sharp increase almost immediately after the partial phases begin to shift to the Gaussian distribution, and they react even more strongly than λ_{20} to the transient changes of the partial phases. In the case of systems *B* and *C* the symmetry parameter S_{20} approaches its maximum possible value (complete symmetry) already at $t \approx 23$ time units. In the case of system *A*, where the amount of induced correlations is considerably lower, the maximum value is reached at time unit 26. The evolution of N_{20}^P allows a better discrimination between the three cases, and as in the case of S_{20}, again the transition is characterized by a drastic increase of N_{20}^p. At the same time the other eigenvectors assume predominantly antisymmetric configurations, as confirmed by a decrease of S_i, $i=1,\ldots,19$ (not shown).

The symmetry properties of the repelling eigenstates can be understood qualitatively by considering a simple matrix model. Let

$$\mathbf{C} = \begin{pmatrix} 1 & c \\ c & 1 \end{pmatrix}; \tag{6}$$

then the eigenvalues of $\mathbf{C}$ are $\lambda_\pm = 1 \pm c$, and the corresponding eigenvectors are symmetrical and antisymmetrical superpositions of the canonical basis vectors $\vec{v}_\pm = (1/\sqrt{2}) \times \left[\binom{1}{0} \pm \binom{0}{1}\right]$, i.e., if $|c| \to 1$, one of the eigenvalues tends to zero while the other one approaches 2 such that the trace of the matrix $\mathbf{C}$ stays constant. Whether $\lambda_+ > \lambda_-$ or vice versa follows from the sign of the correlation coefficient *c*. If $c > 0$ (correlation) $\lambda_+ > \lambda_-$, and the eigenstate corresponding to the larger eigenvalue is a symmetric configuration of the basis states. If anticorrelations are present, $c < 0$, the situation is reversed, i.e., the eigenstate corresponding to the larger eigenvalue has an antisymmetric characteristic. The level repulsion produces a symmetrical and an antisymmetrical mixing of the eigenstates.

At this moment it is worthwhile to make a remark about the proposed interpretation for the number of principal components. Originally N_i^p was introduced as a measure of constructive interference of quantum states, which in a semiclassical picture describe the collective motion of the constituents of a many-particle quantum system (as in the example of giant resonances [23]). In the present case it reflects the increase of the degree of synchronization between different time series. If we understand the $X_i(t)$ as the result of a multivariate measurement of a spatially extended complex system, N_{20}^p measures to what extent the dynamics of the multiple degrees of freedom are synchronized. N_{20}^p is determined by an interference process of the highest eigenstate with others, or, equivalently, by level repulsions of the highest eigenstate with others [24,25]. The mixing between the eigenvectors involved in this process increases gradually during the repulsion process [24]. If all states participate, the distribution of the expansion coefficients a_{ij} becomes uniform, which leads to a maximum value of N_{20}^p [25]. As in many-body quantum systems the number of principal components is a valuable measure for collectivity. It is remarkable that in the present case, where the repulsion between λ_{20} and all other eigenvalues occurs simultaneously, the maximum possible symmetry of $\vec{v}_{20}$ is reached long before all basis states contribute equally to the expansion of $\vec{v}_{20}$. This example implies that the dynamics of the largest eigenvalue reflects the overall dynamics of the system, i.e., the degree of collectivity between all $X_i(t)$.

C. Correlations within a subset of time series

All cases discussed so far illustrate how the spectrum of eigenvalues and eigenvectors reacts if phase correlations are induced in all time series simultaneously. For multivariate data sets it is possible that correlations occur only within a subset of time series. Obviously, the detection of such correlations and the identification of the correlated subsystems is of great practical interest. Therefore, in this section we turn to the analysis of time series generated by system *D* of Table I where correlations are induced between the first two of $M=20$ $X_i(t)$.

Figure 2 gives an overview of the results for the analysis. In the first column [Figs. 2(a), 2(d), and 2(g)] the largest, second smallest, and smallest eigenvalues are shown as functions of time, the second column [Figs. 2(b), 2(e), and 2(h)] displays the results for the number of principal components N_i^p, and the third column [Figs. 2(c), 2(f), and 2(i)] displays the symmetry parameter S_i of the corresponding eigenvectors $\vec{v}_{20}$, $\vec{v}_2$, and $\vec{v}_1$, respectively.

The increase of λ_{20} starting at about 30 time units [Fig. 2(a)] can still be discriminated clearly from the statistical fluctuations. But its increase is much less pronounced than in the cases discussed in Sec. III B. On the average λ_{20} increases by about 12%, from about 1.504 ± 0.025 to 1.68 ± 0.035. On the other hand, in this case the decrease of the smallest eigenvalue is more pronounced. λ_1 decreases by about 25%, from an average value of about 0.588 ± 0.007 during the first 20 time units (first segment) to an average value of about 0.437 ± 0.005 during the last segment. Here, the change of λ_{20} is almost completely compensated by a corresponding change of λ_1. All other eigenvalues, as well as their corresponding eigenvectors, do not show significant

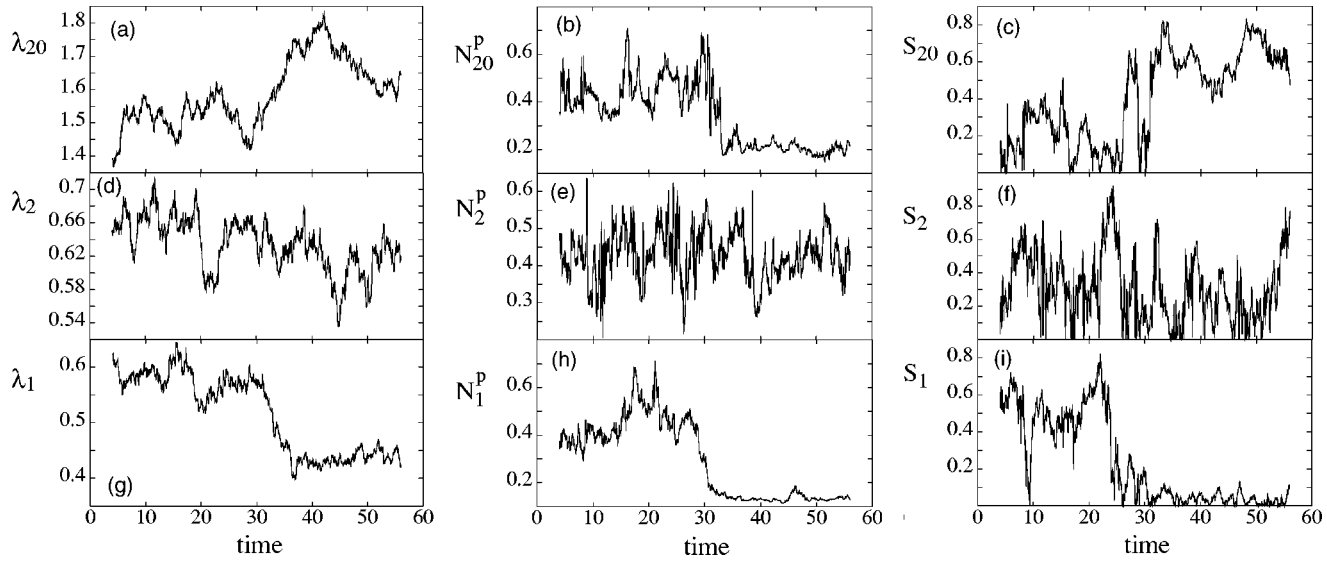

FIG. 2. Results for system *D* of Table I. (a) Largest eigenvalue λ_{20}, (b) number of principal components N_{20}^{p}, and (c) the symmetry parameter S_{20} of the largest eigenvector $\vec{v}_{20}$. (d), (e), and (f) show the corresponding quantities for the second smallest state and (g), (h), and (i) for the smallest state. The time scale is given in arbitrary units as explained in the text.

changes during the transition from the first to the last segment. We found that they remain insensitive to the increase of synchronization within a subsystem of two time series and show only fluctuations around some constant average value, which is determined by the amount of random correlations or equivalently by the finite size of Δt. Exemplary for this part of the spectrum, we show the results for λ_2 and $\vec{v}_2$ in Figs. 2(d)–2(f).

The transient change of the correlation structure is also reflected in the symmetry properties of the eigenvectors. The eigenvector $\vec{v}_{20}$ tends to be more symmetric during the last segment, while $\vec{v}_1$ has a well pronounced antisymmetric characteristic during the same time interval, resulting in a small value of S_1 with tiny fluctuations. On the other hand, the number of principal components of both the smallest as well as the largest eigenvector decreases significantly during the transient central time segment [Figs. 2(b) and 2(h)], indicating that these eigenstates are almost perfectly oriented into a two-dimensional subspace of the 20-dimensional configuration space. In other words, during the last segment the mutual correlations induced in only a small subset of the channels (which define the correlated subspace) provoke substantial changes of the properties of the eigenvectors corresponding to the largest and some of the smallest eigenvalues. The symmetry parameters of the remaining states $\vec{v}_i$, $i=2,\ldots,19$, as well as their numbers of principal components, do not show any significant changes [Figs. 2(e) and 2(f)]. In general, if a subset of $K<M=20$ time series is correlated, we observe that K eigenvalues (and hence their corresponding eigenvectors) react. The largest eigenvalue increases, while the $K-1$ lowest eigenvalues decrease. The strength of the induced correlations and the dimension of the correlated subsystem determine the amount by which the eigenvalues at the edges of the spectrum change.

This behavior can be perfectly explained by the simple matrix model mentioned in Sec. III B. In the present case a level repulsion occurs only between the largest and the smallest eigenvalues (or more generally, in the case of K correlated time series, between the largest eigenvalue and the $K-1$ smallest eigenvalues). Essentially only the eigenstates corresponding to those eigenvalues interfere with each other. This leads to almost purely symmetric and antisymmetric mixing of the components corresponding to the K-dimensional subspace defined by the subset of correlated time series, i.e., only the mutual correlations measured in this subspace give dominant contributions. The remaining states contribute only slightly via the random correlations caused by the finite size of the time window. For this reason, the number of principal components of the largest state decreases, provided that the dimension K of the correlated subsystem is sufficiently small ($K \ll M$). The question which of the time series $X_i(t)$ do synchronize (i.e., do belong to this subspace) can be answered by inspecting the eigenvectors directly.

Figure 3 shows the squared modulus of the eigenvector components of $\vec{v}_1$ [Figs. 3(a) and 3(b)] and $\vec{v}_{20}$ [Figs. 3(c) and 3(d)]. The results in Fig. 3 represent averages over 500 realizations of system *D* (solid lines). Figures 3(a) and 3(c) show the results for uniformly distributed partial phases; Figs. 3(b) and 3(d) are calculated for an N_f-torus with the characteristics of the third segment of system *D*. Dashed lines denote 95% confidence profiles of the distribution of results. While in the case of uncorrelated dynamics an almost uniform distribution of the $|a_{ij}|^2$ with large statistical fluctuations is found, in the case of system *D* for both $\vec{v}_1$ and $\vec{v}_{20}$ dominant components are generated only from the first two $X_i(t)$, i.e., the correlated signals. The statistical fluctuations in the correlated segment are tiny, thereby confirming the significance of this result. As a remarkable detail, the statistical fluctuations of the smallest eigenvector $\vec{v}_1$ [Fig. 3(b)] are even smaller than those of $\vec{v}_{20}$. Statistically, the results obtained for $\vec{v}_1$ have a higher degree of significance, as compared to those obtained for $\vec{v}_{20}$. This might be relevant for highly nonstationary systems, where time averaging is only

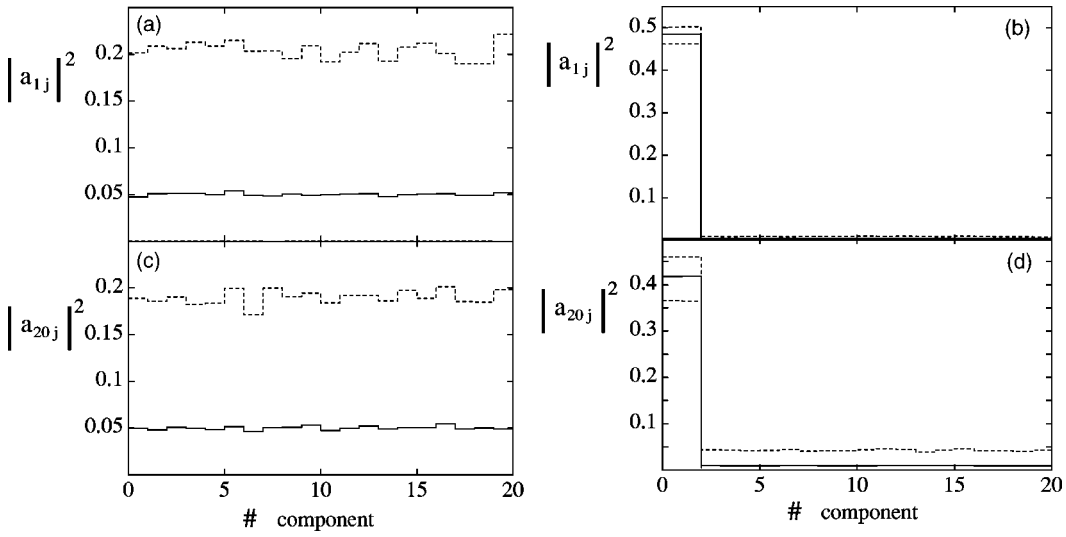

FIG. 3. Distribution of the eigenvector components $|a_{ij}|^2$ for the smallest eigenvector (a) and (b) and for the largest eigenvector (c) and (d). The results in (a) and (c) were calculated for the first segment of system *D* of Table I, while (b) and (d) show the results of the last, correlated segment of system *D*. The solid line is obtained by averaging over 500 different realizations of system *D*. Dashed lines denote 95% confidence profiles.

justified within short periods. All other basis states, representing the remaining time series, participate only weakly in this interference process. During the last segment, the $|a_{ij}|^2$ of the eigenvectors $\vec{v}_i$, $i=2,\ldots,19$, show an almost uniform distribution (resulting from random correlations) with a marginal contribution of the components corresponding to the correlated subspace. Furthermore, they show large statistical fluctuations indicating that these eigenvectors rotate rapidly in the $(M-2)$-dimensional uncorrelated subspace. Thus, the inspection of the eigenvectors yields detailed information about which time series $X_i(t)$ belong to the correlated group.

D. Phase relations between groups of correlated signals

We now turn to the case where groups of time series possess correlations. Here the question arises to what extent it is possible to extract such information from measured multivariate data. N_f-tori easily permit one to simulate situations where certain groups of correlated $X_i(t)$ have different mutual phase relations. In principle, there are two situation of major interest: the dynamics of two groups may be uncorrelated or anticorrelated. For the case of N_f-tori it seems to be inappropriate to interprete $C_{ij}=0$ as evidence for uncorrelated time series $X_i(t)$ and $X_j(t)$, because in the case of harmonic oscillations $C_{ij}=0$ implies a constant and well defined phase difference of $\Delta\delta=\pi/2$ between the time series. In the next section we will justify this interpretation by studying time series produced by autoregressive models.

Figure 4 presents the results for system *E* of Table I, namely, the case of two mutually anticorrelated groups, each of which consists of two correlated time series $X_i(t)$. Figures 4(a) and 4(c) show the time evolution of the largest eigenvalue [Fig. 4(a)] and of the three smallest eigenvalues [Fig. 4(c)]. It can be seen that all eigenvalues shown in the figure react during the transient second segment, where the transition from the uncorrelated to the correlated state takes place: λ_{20} increases while the λ_i, $i=1,2,3$, decrease. The remaining eigenvalues do not show any conspicuous behavior during the whole time course. Comparing these results with the results of the preceding section it appears that by only looking at the eigenvalues one cannot distinguish between the case of four correlated time series and the present case of two mutually anticorrelated groups of correlated time series. Also the number of principal components N_i^p of the largest and the three smallest eigenvectors behaves as in a system of four correlated signals, i.e., similarly as shown in Fig. 2. In Figs. 4(b) and 4(d), the symmetry parameters of the largest eigenvalue [Fig. 4(b)] and of the three smallest eigenvalues [Fig. 4(d)] are shown; here the results are qualitatively different from the previously discussed situations. S_{20} displays on average a considerable decrease with only tiny statistical fluctuations in the correlated third segment. On the other end, S_i, $i=1,2,3$, reveal a trend toward a more symmetric structure, while the remaining eigenvectors $\vec{v}_i$, $i=2,\ldots,19$, again do not show any conspicuous behavior. By investigating the components a_{ij} of the four eigenvectors $\vec{v}_i$, $i=1,2,3,20$, it is possible to directly identify the correlation structure of this multivariate data set. The a_{20j} corresponding to the correlated times series are significantly larger than the others, similar to the case discussed in Fig. 3. They assume values of about ± 0.45, while the remaining coeficients fluctuate between ± 0.1. Furthermore, those a_{20j} corresponding to the two anticorrelated groups have opposite signs. Hence, the sign of the expansion coefficients reveals which pairs among the $X_i(t)$ are mutually correlated or anticorrelated. Thus, detailed information about the transient correlation structure can be retrieved from these quantities.

Again, as in the case discussed in Figs. 2 and 3, there occurs a level repulsion between the highest eigenvalue and only a few smallest eigenvalues. The number of small eigenstates participating in this interference process is given by the total number of correlated time series. Eigenvalues do

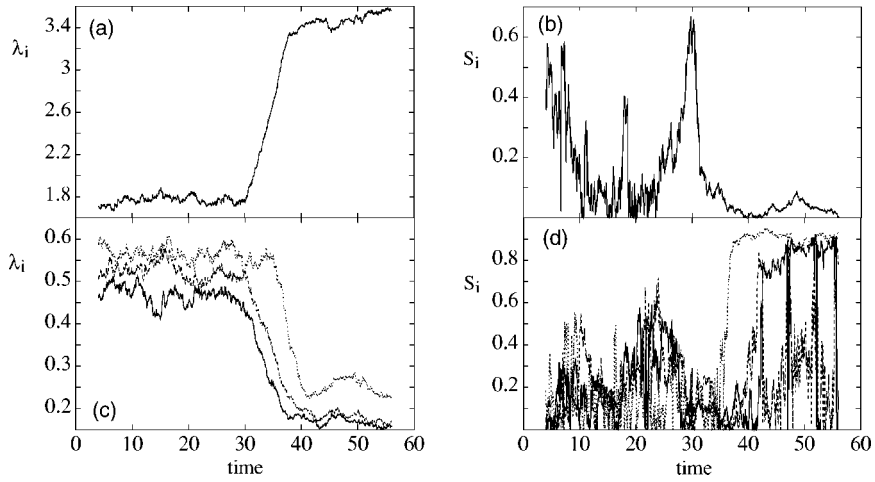

FIG. 4. Results obtained for system *E*, i.e., when two mutually anticorrelated groups of correlated time series are generated each of which contains two time series. (a) shows the time evolution of the largest eigenvalue λ_{20} and (b) the symmetry parameter S_{20} of the largest state. In (c) the results for the three smallest eigenvalues are shown: λ_1 (solid line), λ_2 (dashed line), and λ_3 (dotted line). In (d) the results for the symmetry parameter S_i for the three smallest states are shown, using the same line coding as in (c). The time scale is given in arbitrary units as explained in the text.

not differentiate between correlated and anticorrelated situations; this aspect has to be extracted from the corresponding eigenvectors. The correlation matrix assumes a block-diagonal form with positive correlation coefficients inside each block on the diagonal, while the nondiagonal matrix elements connecting the two blocks have mostly negative signs. In terms of the simple matrix model Eq. (6) this corresponds to the case $c<0$. The sharp local maximum that can be seen at about 30 time units in Fig. 4(b), is caused by the crossing of the partial phases during the shift from the uniform to the Gaussian distribution. During this transition the distribution of the partial phases becomes narrower, while it is not yet showing two maxima displaced by a phase difference $\Delta\delta=\pi$. Therefore, transiently the four time series become highly correlated, resulting in a symmetric structure of $\vec{v}_{20}$, in accordance with model Eq. (6).

System *F* of Table I is a realization for two uncorrelated groups of $X_i(t)$, i.e., the maxima of the Gaussian distributions of random partial phases are displaced by a phase difference $\Delta\delta=\pi/2$. Figure 5 shows the results of the analysis of time series corresponding to system *F*. Figures 5(a) and 5(c) show the two largest and the two smallest eigenvalues, respectively. In Figs. 5(b) and 5(d) the corresponding results for the symmetry parameter are shown. The largest eigenvalue λ_{20} shows a clear increase with a well pronounced maximum at about 30 time units during the transient segment, where due to the crossings of the partial phases the width of the phase distribution assumes a minimum, thereby causing strong correlations, while the two groups are not yet distinguishable. Also λ_{19} starts to increase, such that in the final segment the two largest eigenvalues fluctuate at values slightly above 2. Correspondingly, the two smallest eigenvalues decrease, in

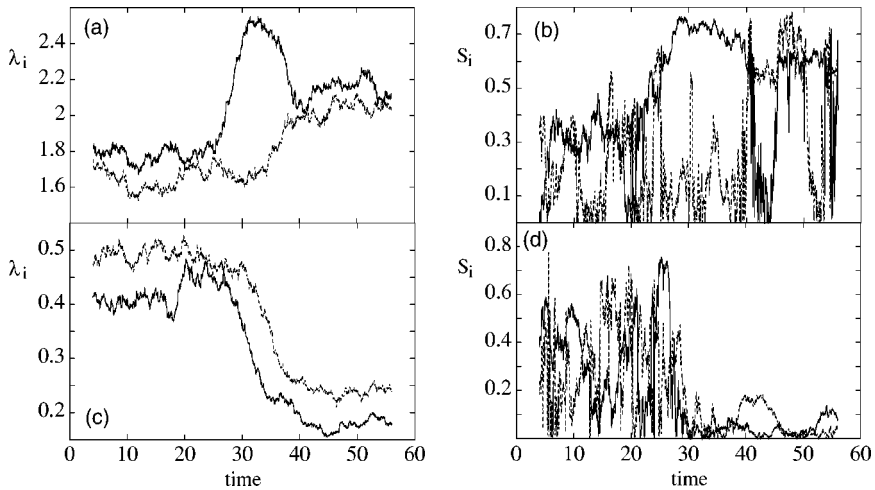

FIG. 5. Results obtained for system *F*, two mutually noncorrelated groups of correlated time series are generated. (a) shows the time evolution of the largest eigenvalue λ_{20} (solid line) and the second largest eigenvalue (dashed line). In (b) the symmetry parameters S_{20} of the largest state (solid line) and S_{19} of the second largest eigenvector (dashed line) are shown. In (c) the results for the two smallest eigenvalues are shown: λ_1 (solid line), λ_2 (dashed line). In (d) the results for the symmetry parameter S_i for the two smallest states are shown, using the same line coding as in (c). The time scale is given in arbitrary units as explained in the text.

order to satisfy the condition of trace invariance of **C**. All other eigenvalues λ_i, $i=3,\ldots,18$, essentially do not participate in this process. The structure of the correlation matrix during the correlated time segment shows two blocks (one for each of the correlated groups) which are essentially disconnected, i.e., on the average the C_{ij} connecting both blocks are zero. Geometrically this means that the repelling eigenstates (the states affected by the correlations) assume an almost orthogonal orientation with respect to the basis vectors of the uncorrelated subspace. Furthermore, each of the two largest eigenstates tends to an almost orthogonal position with respect to the correlated subspace defined by one of the two groups. In the limiting case of two completely uncorrelated groups, each containing ten perfectly correlated (identical) time series, **C** assumes a block-diagonal form with two 10×10 blocks with $C_{ij}=1$ inside each block, while the remaining nondiagonal matrix elements are equal to zero. Hence, this system splits up into two independent ten-dimensional subsystems. Consequently, there arise two large eigenvalues, one for each subsystem, each with a value of 10, while all other eigenvalues tend to zero.

In Figs. 5(b) and 5(d), the symmetry parameters of the two largest eigenvalues [Fig. 5(b)] and those of the two smallest eigenvalues [Fig. 5(d)] are shown. It can be seen that the two largest eigenvalues tend toward symmetric compositions of the basis states. As a result of the phase crossings during the second segment transiently only λ_{20} shows a well pronounced symmetric structure. The nondiagonal matrix elements of **C** connecting the two blocks are not zero. Therefore, the two groups are not perfectly independent. This leads to a weak mixing of the two largest eigenstates even during the correlated last segment, and consequently fluctuations of S_i, $i=19,20$, appear starting from time unit 40. On the other hand, the structure of the states of the two smallest eigenvectors shows clearly antisymmetric characteristics.

In [28] a group model was proposed in order to explain the appearance of several large eigenvalues deviating from the RMT predictions. The authors proposed that the empirical correlation matrix of [10,11] had block-diagonal form, each block representing a set of companies belonging to the same kind of industry or market sector. A similar conclusion was drawn in [14], where it was proposed that certain subsets of stocks were formed, corresponding to companies from the same "conventionally identified" business sectors. Eguiliz and Zimmermann have presented a model for opinion cluster formation and information dispersal by agents in a network [29]. The transmission of information within the network of all traders follows a random process, such that groups of agents are formed in a self-organized manner (herding). In this context "herding" means that agents are not making decisions individually, but instead agents belonging to the same group perform collective actions, i.e., strong correlations are present between the agents of each group. We suggest that this type of collective behavior of certain subsystems can be well described by the mechanisms discussed in Figs. 4 and 5.

Concluding this section, we can state that the time-resolved spectrum of eigenvalues and eigenvectors of **C** provides detailed information about the changes of the correlation structure of multivariate time series data, in terms of level repulsions between a certain number of states. Groups of correlated time series $X_i(t)$ are detected, as well as details of the relationship between correlated subsystems. If in total K time series become correlated, K eigenvalues at the edges of the spectrum increase or decrease, respectively. The structure of the corresponding K eigenvectors provides detailed information about which $X_i(t)$ gets correlated. Furthermore, the symmetry parameter $S_i(t)$ tells whether synchronization or antisynchronization is present.

IV. MULTIVARIATE AUTOREGRESSIVE PROCESSES

The class of N_f-tori discussed so far represents a deterministic testing system for which phase correlations can be induced in a precisely controllable way. In order to put the obtained results onto more general grounds, we will now investigate time series generated by autoregressive models, i.e., a class of stochastic dynamical system.

A. Definition and design of the system

Linear autoregressive processes have been among the most popular and useful dynamic models for time series analysis for a long time [30]. The multivariate generalization of autoregressive processes (MAR) is given by

$$y_i(t_n)=\sum_{s=1}^{p}\sum_{j=1}^{N_y}A_{ij}(s)y_j(t_n-sT)+\eta_i(t_n),\quad i=1,\ldots,N_y, \tag{7}$$

where p denotes the model order, N_y the state dimension, and T the unit of discrete time. The $A_{ij}(s)$ are a set of $N_y\times N_y$ parameter matrices, and $\eta_i(t_n)$ is an N_y-dimensional time series of Gaussian white noise. By defining an augmented new state vector consisting of the actual state vectors at time points $t_n,(t_n-T),\ldots,[t_n-(p-1)T]$, it is always possible to transform a MAR model of order p into a first-order MAR model; this is known as a state-space approach and corresponds to time-delay embedding. In this case only one parameter matrix of size $pN_y\times pN_y$ is required. The noise terms $\eta_i(t_n)$ for these additional time-delayed state variables are set to zero. Here we employ a special class of first-order MAR models, defined by the $2N_y\times 2N_y$ parameter matrix

$$A_{ij}=\begin{cases}2\,\mathrm{Re}(\lambda_n) & \text{if } i=j \text{ and } i=2n-1,\\ -|\lambda_n|^2 & \text{if } i=j-1 \text{ and } i=2n-1,\\ 1 & \text{if } i=j+1 \text{ and } i=2n,\\ 0 & \text{otherwise.}\end{cases} \tag{8}$$

Here λ_n, $n=1,\ldots,N_y$, denotes a set of complex numbers which are generated by choosing their partial phases from a uniform distribution within $[0,\pi/2]$ and their moduli from the asymmetrical distribution $p(|\lambda|)\propto|\lambda|^4(1-|\lambda|^4)$ within [0, 1]. The set of the λ_n and their complex conjugates represent the characteristic roots of the MAR models, i.e., they describe its frequency response. Moduli should not exceed unity, otherwise the model would become unstable. The λ_n were chosen from the first quadrant with a probability distribution that peaks close to unity but becomes zero at unity. The resulting model is equivalent to a set of N_y uncoupled

univariate second-order AR models ($p=2$) which are accommodated into a $2N_y$-dimensional state-space model; each AR(2) model performs a stochastic oscillation with an individual frequency and an individual width of its spectral peak. Note that only those $\eta_i(t_n)$ with odd indices $i=2n-1$ will be nonzero, since the other positions correspond to time-delayed variables.

Now we assume a set of M of these MAR processes with state vectors $y_{ik}(t_n)$, $i=1,\ldots,N_y$, $k=1,\ldots M$, all simultaneously active, each driven by a noise process $\eta_{ik}(t_n)$. We can introduce couplings into these processes by choosing these noise processes as

$$\eta_{ik}(t_n) = c(\rho)[\rho\xi_i(t_n) + (1-\rho)\tilde{\chi}_{ik}(t_n)], \tag{9}$$

where $\xi_i(t_n)$ is a (multivariate) noise process common to all MAR processes, whereas $\tilde{\chi}_{ik}(t_n)$ is a set of (multivariate) noise processes that is uncorrelated with respect to the index k; both processes are chosen as zero-mean unit-variance Gaussian white noise. The parameter ρ determines the degree of correlation between the individual MAR processes; $\rho=0$ corresponds to completely uncorrelated processes, while for $\rho=1.0$ all processes are driven by the same noise process and therefore produce identical time series. $c(\rho)$ denotes a normalization function which ensures that the variance of the sum of the two independent noise processes $\xi_i(t_n)$ and $\tilde{\chi}_{ik}(t_n)$ remains unity.

Finally the N_y-dimensional state vector of each MAR process is mapped to a univariate observation by summation over all second-order AR models, i.e.,

$$X_k(t_n) = \sum_{n=1}^{N_y} y_{2n-1,k}(t_n). \tag{10}$$

This summation corresponds to the summation in Eq. (5). However, instead of generating time series with a broad power spectrum by summing up a set of sine waves, we sum up a set of stochastic (i.e., intrinsically broadbanded) oscillations. Correlations are not induced by correlated partial phases, but by driving the stochastic oscillations with correlated noise.

Again we create multivariate time series with time dependent change of the correlation structure by sampling 20 time units (first segment) from an uncorrelated system (where $N_y=100$ and $M=20$), after allowing for an initial transient to die out; then ρ is linearly increased from 0.0 to 0.5 over another 20 time units, while continuing the sampling of the system (second segment). Finally ρ is kept constant at a value of 0.5, while another 20 time units are sampled (last segment). This correlation may be imposed to all MAR processes, or only to subsets chosen from the set of all MAR processes. It is also possible to generate several subsets of correlated processes, such that the dynamics of each subset remain uncorrelated to the dynamics of other subsets, similar to the situation of system F for the case of N_f-tori. For this class of systems we explicitly discuss only cases where the correlations are confined to such subsets.

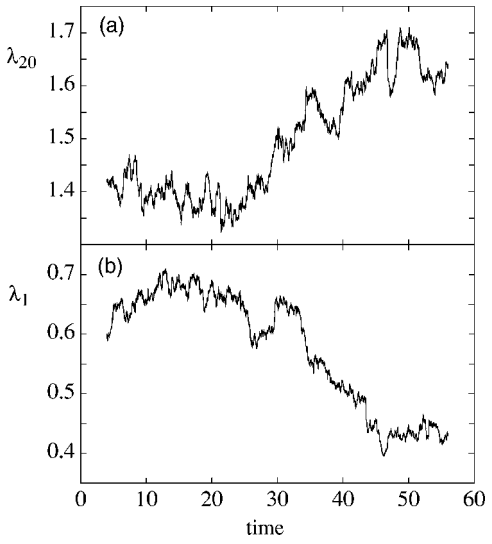

FIG. 6. Time development of (a) the largest eigenvalue λ_{20} and (b) the smallest eigenvalue λ_1 for the MAR model Eq. (7), when only two from $M=20$ time series are correlated via the noise mixing described by Eq. (9) with $\rho=0.5$. The time scale is given in arbitrary units as explained in the text.

B. Correlations within a subset of time series

Because the case when all M time series get correlated is the most trivial one we focus in the following only on those systems where the correlation structure of certain groups of channels is changed. As a first example we present the result for the case where only two from $M=20$ time series were correlated with $\rho=0.5$. The results for the largest and smallest eigenvalues are displayed in Fig. 6. As in the case of N_f-tori, only the largest and the smallest eigenvalues react noticeably to the transient change of correlation structure. Again, λ_{20} increases already in the second segment, while λ_1 tends toward lower values; all other eigenvalues do not show any conspicuous behavior. The change of correlation structure results in a level repulsion of the corresponding eigenvalues. The number of eigenstates involved is given by the number of correlated time series. Similar to the case of N_f-tori presented above, detailed information on the question of which of the time series become correlated can be obtained from investigating the structure of the eigenvectors directly.

In order to check the sensitivity of the method in the case of MAR systems and to verify the statistical significance of the results, we performed the following numerical experiment. We increased ρ successively from zero to 1 in steps of 0.04. For each value of ρ we performed 100 runs, each time creating $M=20$ time series each of length 8 time units, which we then analyzed by forming the correlation matrix of the whole time series ($\Delta t=8$). The results are shown as a function of ρ in Fig. 7 for the case when only two out of 20 time series are correlated [Fig. 7(a)], and for the case when two groups of two time series each are correlated, but no correlations exist between these two groups [Fig. 7(b)]. Two mutually uncorrelated groups of correlated time series can readily be generated by employing two statistically independent noise terms $\xi_i^1(t_n)$ and $\xi_i^2(t_n)$, one for each group [com-

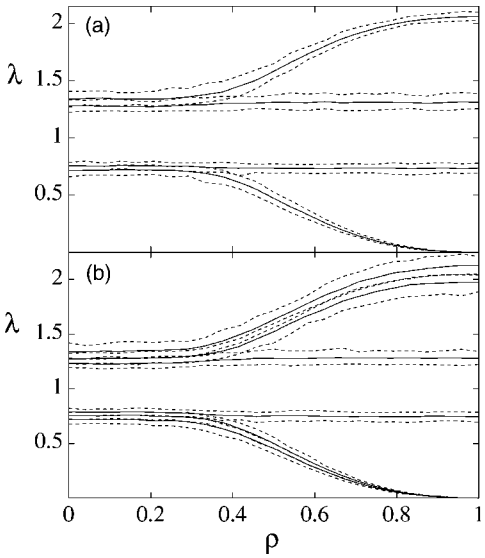

FIG. 7. Eigenvalues as a function of ρ for the MAR model Eq. (7), for the case when (a) only two from $M=20$ time series are correlated via noise mixing described by Eq. (9), and (b) two mutually uncorrelated groups are generated, each group containing two time series. The figure displays the average value taken over 100 trials for each ρ (solid lines) and 95% confidence profiles (dashed lines). In (a) the two largest and the two smallest eigenvalues are shown as functions of the mixing parameter ρ [see Eq. (9)]. (b) shows the same for the three largest and three smallest eigenvalues.

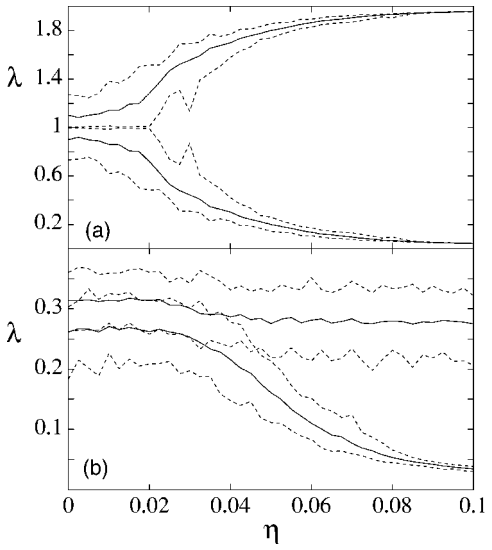

FIG. 8. η dependence of the eigenvalues of the correlation matrix calculated from time series of the coupled Rössler system Eq. (11). An average over 100 trials for each value of η with different initial conditions is shown (solid line). Dashed lines denote 95% confidence profiles; (a) the two eigenvalues for $M=2$ coupled Rössler systems; (b) the two smallest eigenvalues when only two from a total of $M=20$ systems [Eq. (11)] are coupled.

pare Eq. (9)]. Figure 7 also shows the magnitude of statistical fluctuations by displaying 95% confidence profiles (dashed lines). Note that in the case of MAR processes as defined above, it is justified to speak of "uncorrelated groups," since there is no longer an average phase shift of $\pi/2$ between groups.

In Fig. 7, we find qualitatively similar behavior as in the corresponding case for N_f-tori. If only two time series are correlated, the largest eigenvalue increases and the smallest eigenvalue decreases. The values of λ_i, $i=2,\ldots,19$, remain unchanged. The stronger the correlation of the $X_i(t)$, the more pronounced is the separation of λ_{20} and λ_1 from the bulk. If two mutually uncorrelated groups are formed, the two largest eigenvalues tend to values close to 2, while the two smallest eigenvalues decrease to zero [Fig. 7(b)]. The behavior of the corresponding eigenvectors is similar to that shown in Fig. 5. When increasing ρ, $\mathbf{C}$ tends to have block-diagonal form, where those elements C_{ij} connecting the two blocks are vanishing. Hence, two independent interference processes are present, each of which generates a large eigenvalue. By this mechanism the occurrence of more than one large eigenvalue well separated from the bulk, as observed in [10–14], can be perfectly explained.

V. COUPLED CHAOTIC SYSTEMS WITH FUNNEL ATTRACTOR

In [31] a system of two coupled Rössler oscillators was discussed as an example of a system for which phase correlations, resulting from increasing coupling strength, can hardly be detected. The authors proposed a method employing auxiliary oscillators which are driven by the system. From the responses of these auxiliary oscillators the degree of phase synchronization could be retrieved. Now we would like to consider this system in a generalized version, in order to demonstrate that for this system the methodology presented in this paper provides an improved sensitivity for the detection of phase correlations while requiring less computational effort.

The system discussed in [31] is defined as follows:

$$\dot{X}_{1,2} = -\omega_{1,2}Y_{1,2} - Z_{1,2} + \eta(X_{2,1} - X_{1,2}),$$

$$\dot{Y}_{1,2} = \omega_{1,2}X_{1,2} + \beta Y_{1,2} + \eta(Y_{2,1} - Y_{1,2}),$$

$$\dot{Z}_{1,2} = 0.1 + Z_{1,2}(X_{1,2} - 8.5), \tag{11}$$

with $\omega_1=0.98$, $\omega_2=1.03$, and $\beta=0.28$. η denotes the coupling strength between the two Rössler systems.

Using Eq. (11) as a basic unit describing a pair of coupled systems, we performed two numerical experiments. First we consider $M=2$ coupled oscillators [i.e., one pair, as described by Eq. (11) with nonzero η], then a set of $M=20$ systems, where only the first two are coupled as described by Eq. (11) with a nonzero value of η, while the $M-2$ remaining systems stay uncoupled ($\eta=0$). We generate a multivariate time series by sampling the X components of each system. Then we increase η from 0.0 to 0.1 in steps of 2.439×10^{-4}, creating for each value of η 100 time series of length $\Delta t=8$ time units with different initial conditions. The results of the analysis of this system are displayed in Fig. 8. Figure 8(a) shows the eigenvalues λ_1 and λ_2 as functions of η for the

case of $M=2$ coupled oscillators. The solid lines denote averages over the 100 trials; the dashed lines denote 95% confidence profiles. We find a smooth transition from the uncorrelated case $\eta=0$ to an almost perfect phase synchronization at $\eta=0.1$.

Figure 8(b) displays the corresponding results for the two smallest eigenvalues λ_1 and λ_2 for the case of two out of a total of 20 Rössler systems being coupled. A clear separation between these two lowest states can be seen, increasing monotonically with increasing η. Due to a larger amount of random correlations within the 20-dimensional data set, the point of separation is found at a somewhat larger value of η, as compared to the case of only two coupled oscillators [shown in Fig. 8(a)]. Nevertheless, the method succeeds in sorting out the essential features of the correlation structure of this multivariate time series. All other eigenvalues, including the largest one, do not display any significant changes while η is increased. The essential information about the phase synchronization of these time series can be extracted *only* from the dynamics of the lowest eigenvalues. These eigenvalues react much more sensitively than the largest eigenvalue, which is governed mainly by global changes of the spatiotemporal correlations. Again detailed information about which of the oscillators are communicating via the coupling term in Eq. (11) can be obtained directly from the structure of the corresponding eigenvectors, as already described above.

VI. COMPARISON WITH OTHER METHODS

In this section we would like to compare the performance of the approach based on the equal-time correlation matrix with other methods designed for related tasks of time series analysis. All nonstationary time series employed in this paper, generated either by the systems listed in Table I, by the MAR model, or by coupled Rössler systems, display no noticeable changes of their spectral composition. In principle, the gradual changes of the partial phases that occur in the second segment of the N_f-tori time series are equivalent to adding a time dependent frequency component to the randomly chosen, but otherwise constant, frequencies f_i in Eq. (5). This should be reflected in the power spectrum of the corresponding time series, such that some hints about the nonstationary character of the $X_i(t)$ could possibly be extracted. However, a careful Fourier analysis of all the corresponding nonstationary time series, using different sizes of the sliding window, did not reveal conclusive evidence for the presence of transient changes. Methods based on the Fourier transform are not sensitive to changes in the phase relations between time series.

A method designed particularly for the purpose of detecting phase relationships between time series is the Hilbert transform [7]. It is based on extracting the instantaneous phases $\Phi_i(t)$ of the time series $X_i(t)$, $i=1,\ldots,M$, via convolution with the function $f(t)=1/t$. In order to detect any possible increase of phase locking between the $X_i(t)$, the $M(M-1)/2$ different pairs of phases $(\Phi_i(t),\Phi_j(t))$, which can be extracted from an M-dimensional multivariate time series, need to be compared. However, in the case of time series having a broad power spectrum without any dominant frequency component, as is the case for the N_f-tori or the MAR model, the resulting instantaneous phases have no physical meaning [6]. And the coupled Rössler systems display attractors with funnel characteristics for the chosen value of the parameter β in Eq. (11), thereby inhibiting the application of the Hilbert transform [31]. For these reasons we state that the Hilbert transform is not applicable to the examples discussed in this paper.

More promising seems the application of methods that have been developed particularly for the analysis of multivariate time series: principal component analysis [22] and its generalization, independent component analysis (ICA) [8]. The aim of the ICA approach is to find a new representation of the data $X_i(t)$, such that a set of M (or fewer) new time series is estimated from the data, each of them displaying the activity of an independent source process. For this purpose, the M-dimensional phase space which is formed by the multivariate time series $X_i(t)$, $i=1,\ldots,M$, is considered. One tries to find a set of (not necessarily orthogonal) linear independent vectors, such that the projection of the data onto the direction given by each of these vectors is least Gaussianly distributed, or, in other words, one tries to find directions that provide maximal information. In order to investigate the performance of ICA for the detection of time-varying correlation structure, we employed the FASTICA algorithm. For this purpose we use the FASTICA MATLAB package provided by the Neural Network Research Center of the Helsinki University of Technology [32]. We analyzed time series generated from each of the systems based on N_f-tori, as listed in Table I. Similarly we studied the Rössler system when the coupling between two of 20 oscillators was changed from $\eta=0$ to 0.05. For none of these cases do the independent components reflect appropriately the transient changes of the synchronization level. Although the ICA method is known to be successful in other applications, it fails for the systems discussed in this paper, because the joint distribution of the data points $X_i(t_k)$, generated from the systems listed in Table I, resembles very much the joint distribution of Gaussianly distributed random variables, whence it does not contain sufficient information to be exploited by ICA.

VII. EPILEPTIC SEIZURES AS AN EXAMPLE OF GLOBAL COLLECTIVE DYNAMICS

As an example for a globally changing correlation structure in an experimental data set, we now discuss the analysis of an electroencephalographic recording of an epileptic crisis. It is known that during epileptic seizures of petit mal type the activity of a large fraction of the cortical neurons is synchronized [33], and the multivariate EEG time series displays oscillations of comparatively large amplitude and well defined frequency close to 3 Hz. Figure 9(a) presents a segment of 110 s length chosen from a standard EEG recording from a 10-year-old male patient with absence seizures. The time series represents the electrical potential at electrode Pz versus the average of the electrodes F3 and F4 (referring to the standard 10–20 system of clinical EEG electrode terminology). The data were sampled by 12-bit analog-to-digital

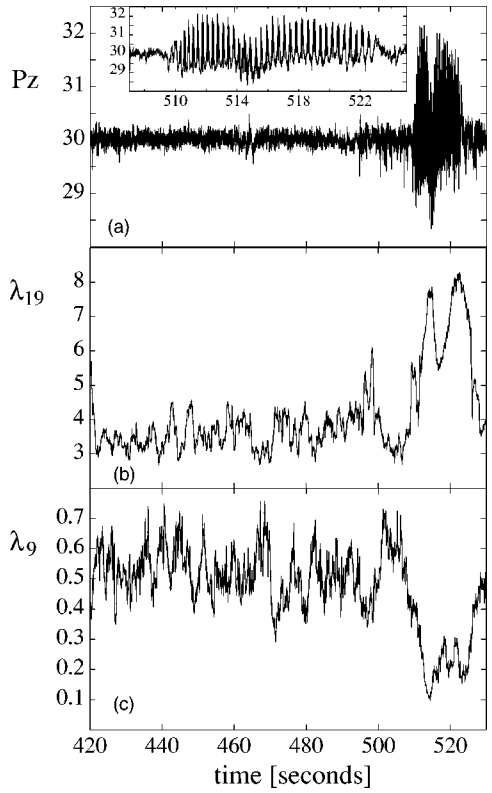

FIG. 9. (a) A segment of 130 s from an EEG recording at electrode Pz. From about 510 to 522 s the large amplitude activity of a generalized epileptic seizure can be seen. The inset magnifies the seizure activity. The time development of (b) the largest eigenvalue λ_{19} and (c) the smallest eigenvalue of the correlation matrix are shown.

conversion at a sampling rate of 256 Hz; no further preprocessing of the data from 19 electrodes was performed.

The first 420 s of the complete recording are not shown, but the time units on the horizontal axis refer to the complete recording. This data set can be regarded as typical of electroencephalographic measurement obtained in clinical practice. From 420 to 510 s the recording shows seizure-free activity which is characterized by irregular fluctuations of the electrical potential. Within the time interval 510–522 s [magnified in the inset of Fig. 9(a)] a pronounced seizure [33] can be seen. The time series recorded at the 18 other electrodes (not shown in the figure) display similar wave shapes during the seizure.

At the onset of the seizure a sudden change of the brain dynamics occurs from a nearly uncorrelated to a highly correlated state covering almost the whole cortex, such that at each electrode almost periodic spike-wave complexes with high amplitude and a frequency close to 3 Hz can be observed. Hence, strong correlations are induced globally in the whole multivariate time series, similar to the examples of systems *A*, *B*, and *C* of Table I. We analyzed this recording using the correlation matrix which was constructed over a moving window of length $\Delta t=2$ s (corresponding to 512 data points). This window was shifted with maximum overlap over the whole EEG recording, and the time evolution of the eigenvalues was computed. The results for the largest eigenvalue λ_{19} are shown in Fig. 9(b). In the preseizure period λ_{19} fluctuates around a comparatively small value, indicating the irregular, almost uncorrelated normal brain dynamics. As soon as the epileptic seizure initiates, λ_{19} rises to significantly larger values, thereby repelling almost the entire rest of the spectrum, which provokes simultaneously a pronounced decrease of the eigenvalues λ_i, $i=1,\ldots,16$. The eigenvalues λ_{17} and λ_{18} do not show any conspicuous behavior before or during the seizure. As an example for the evolution of the smaller eigenvalues, λ_9 is shown in Fig. 9(c).

It can be seen that within the seizure approximately at 515 s λ_{19} assumes a local minimum, its value dropping from almost 8 to about 5.5, and that there is a corresponding local maximum of λ_9 close to this time point; this effect results from an eye movement artifact [see also the inset of Fig. 9(a)], which disturbs the periodic characteristics of the seizure EEG at some of the 19 electrodes. Consequently, a transient loss of correlation is detected.

In [25] this particular type of evolution of the eigenvalue spectrum, i.e., the transition to a repulsion of one eigenstate by all others, was identified as a second-order phase transition. This indicates that the sudden change from the largely irregular dynamics of the normal brain activity to a highly ordered behavior during the seizure state might be explained by the abrupt characteristics of a phase transition. The results in [25] were obtained for the more general case of complex non-Hermitian matrices, but can be directly applied to the real symmetric case. This agrees well with the conclusions drawn in [34] that the spontaneous transition from the irregular normal behavior to the highly correlated dynamical state of an absence seizure can be interpreted as a nonequilibrium phase transition.

VIII. CORRELATION MATRICES AND RANDOM MATRIX THEORY

Random matrix theory was originally developed by Wigner, Dyson, Mehta, and others for the purpose of describing the statistical properties of neutron resonances of complex nuclei with a large number of degrees of freedom [20,35–37]. The main idea was to replace the exact quantum-mechanical Hamiltonian by a matrix composed of independent random elements, drawn according to a prespecified probability distribution. This implies an average over all possible interactions between the members of a many-particle system. This approach turned out to be very successful for the statistical description of nuclear spectra [35,36,38,39] and provided the theoretical basis for a new research field, the physics of quantum chaos [40]. Using the mathematical apparatus of RMT, universal statistical properties of a variety of physical systems could be compared and classified.

Properties of interest in RMT are correlations within the spectrum of eigenvalues of a given Hamiltonian matrix. The two most prominent measures are the nearest-neighbor distribution $P(s)$ and the number variance $\Sigma^2(l)$ [20,39–41]. The application of these measures requires the transformation of the level density ρ to a uniform distribution; this procedure is known as "unfolding" [39,41]. To this end, one calculates the so called accumulated level density

$$N(\lambda) = \int_{-\infty}^{\lambda} \rho(\lambda')d\lambda'. \tag{12}$$

$N(\lambda)$ counts the number of states in the interval $[-\infty,\lambda]$. It can be split into a smooth and a fluctuating part,

$$N(\lambda) = N_{\text{smooth}}(\lambda) + N_{\text{fluct}}(\lambda). \tag{13}$$

Because the fluctuating part

$$\rho_{\text{fluct}}(\lambda) = \frac{dN_{\text{fluct}}(\lambda)}{d\lambda} \tag{14}$$

vanishes on the average, the average level density is solely given by

$$\rho_{\text{smooth}}(\lambda) = \frac{dN_{\text{smooth}}(\lambda)}{d\lambda}. \tag{15}$$

If the smooth part of the accumulated level density $N_{\text{smooth}}(\lambda)$ is known, the eigenvalues Λ_i of the unfolded spectrum are obtained by

$$\Lambda_i = N_{\text{smooth}}(\lambda_i). \tag{16}$$

Hence, the crucial problem of unfolding a spectrum is to find the correct form of $\rho_{\text{smooth}}(\lambda)$. Especially if the analytical formula for the smooth part of the level density is unknown, one has to perform a fit of the numerical probability distribution of the eigenvalues. A common procedure is a polynomial fit to the numerically obtained accumulated level density $N(\lambda)$. This fit function is then used to perform the unfolding transformation [41]. Then correlation functions like $P(s)$ or $\Sigma^2(l)$ are extracted numerically from the unfolded spectrum and are used for comparison with the analytical results derived from random matrix ensembles.

The general problem of extracting and interpreting correlations from data is not limited to the case of spectra of complex quantum systems [38–41], but is of great interest for the analysis of time series arising in various other fields, such as finance data [10–15], magnetoencephalographic and electroencephalographic recordings [17,16,19], or climate data [18]. In these fields the basic laws governing the dynamics are not known (as in the case of the exact Hamiltonian in nuclear physics). Nevertheless it is possible to start from the very general assumption that the dynamics of such systems is composed of a multitude of source processes forming subsystems of different size which may or may not be correlated among each other. It results that in the above-mentioned studies a surprisingly good agreement between the statistical properties of the eigenvalue spectrum of the empirical correlation matrices and those of random Hamiltonians represented by real symmetric matrices was found. The set of random matrices is known as the Gaussian orthogonal ensemble (GOE), i.e., the ensemble of matrices which is invariant under orthogonal transformations.

Strictly speaking, the empirical correlation matrix **C** neither describes the dynamics of a complex quantum system (as Hamiltonian matrices do) nor belongs to the Gaussian orthogonal ensemble. From this point of view, it seems inconsistent to compare the statistical properties of the spectra of **C** with the analytical results obtained for the GOE. A better reference point is the so called Wishart distribution [14,21,42], i.e., an ensemble of correlation matrices constructed over a time interval Δt from M independent time series of normally distributed random values. The statistical properties of the latter differ slightly from those of the GOE, in particular for the part of the spectrum of eigenvalues that lies close to zero. But because these differences decay rapidly with increasing distance from zero, and the upper part of the spectrum is described well by the universal properties of the GOE [14], the comparison seems to be justified.

In [14] it was assumed that the theoretically known expression for the level density of the Wishart ensemble can be used for the unfolding procedure (16). In the limit $M\to\infty$ and $\Delta t\to\infty$, such that $Q=\Delta t/M$ stays constant, the probability distribution of the eigenvalues of the Wishart ensemble is given by [42]

$$P_W = \frac{Q}{2\pi}\frac{\sqrt{(\lambda_+ - \lambda)(\lambda - \lambda_-)}}{\lambda}. \tag{17}$$

In Eq. (17) $\lambda_\pm$ are the largest and smallest eigenvalue of the Wishart matrix given by

$$\lambda_\pm = 1 + \frac{1}{Q} \pm 2\sqrt{\frac{1}{Q}}. \tag{18}$$

For finite values of M and Δt deviations occur at both edges of the spectrum [43]. Using $\lambda_\pm$ and the number of time series of the multivariate data set M as fit parameters the smooth part of the accumulated level density is obtained which has been used for the unfolding procedure in [14]. In principle, neither $\lambda_\pm$ nor the number of time series M of the multivariate data set are free parameters; however, the resulting fit might describe satisfactorily the level density of the empirical correlation matrix.

Applying the concepts of RMT to the analysis of empirical correlation matrices, it was observed that some of the largest eigenvalues showed clear deviations from the RMT predictions. In a number of studies it was concluded that only these largest eigenvalues "contain real information" which cannot be described by random matrices, whereas all other eigenvalues (the "bulk") were essentially dominated by noise, i.e., represented "random correlations" [10,12,13,15,16,19]. Recently this view was questioned by Malevergne and Sornette [44] who demonstrated by explicit statistical testing that also the level density of the "bulk" of eigenvalues deviates slightly from the predictions of the Wishart ensemble Eq. (17); in contrast to the earlier claims they concluded that "there is relevant information also in the bulk of the eigenvalue spectrum."

However, the correlation measures applied in [11–16,18,19] do not depend on the particular form of the level density. On the contrary, systems with quite different level densities might have identical correlation structures in their eigenvalues and different systems with the same eigenvalue distribution might show drastically different correlation properties. Moreover, in order to deduce such correlations from given spectra, one has to remove any particular

properties from the level densities by the unfolding transformation (16) in order to put different spectra on the same footing.

Therefore, an essential step for the extraction of the correlations within a spectrum of eigenvalues is the unfolding procedure (16). Regardless of which strategy is used to adjust some fitting function to the empirical data, in any case major discrepancies between the fit function and the data will occur at both edges of the spectrum. For this reason a thorough analysis takes only the central part of the level density into account for the calculation of correlation measures like $P(s)$ or $\Sigma^2(l)$ [20,39–41]. Among the previous studies which have applied the concepts of the random matrix theory to the analysis of empirical correlation matrices [12,13,15,16,19] none has stated explicitly how many states were omitted at the edges of the level density, before calculating the correlation measures. Nevertheless, the conclusion that *all* eigenvalues belonging to the bulk follow the RMT prediction and hence do not contain any relevant information has not yet been seriously challenged.

The examples discussed in this paper prove the contrary. The key argument of the method is that the increase of synchronization between a number of time series leads to a level repulsion of states at both borders of the spectrum. Because of the invariance of the trace under orthogonal transformation the relative change of the eigenvalues is much larger at the lower edge of the spectrum than at the upper edge (compare the discussion of Fig. 2). Moreover, as in the case presented in Fig. 8(b), there exist situations where the essential information can be extracted only from the states belonging to the smallest eigenvalues. Hence, from a statistical point of view the information drawn from the smaller eigenvalues is more relevant. This conclusion is also confirmed by the results shown in Figs. 3(b) and 3(d), where the structure of the eigenstates corresponding to the largest and the smallest eigenvalues are compared for the case where only two from a total of 20 time series being correlated. $\vec{v}_1$ as well as $\vec{v}_{20}$ assume an orientation almost to the subspace defined by the two correlated time series while the magnitude of all remaining components is of negligible size. The essential information about the correlation structure of the multivariate time series is imprinted in both eigenstates. However, the statistical fluctuations of $\vec{v}_{20}$ are considerably larger than those of $\vec{v}_1$. Hence, the lower part of the spectrum of **C** does contain relevant information about the correlation structure of a multivariate data set.

IX. SUMMARY AND CONCLUSIONS

The numerical examples presented in this paper demonstrate the utility of using the spectrum of eigenvalues and eigenvectors of the equal-time correlation matrix for the analysis of nonstationary multivariate time series. The most important features of the presented approach can be summarized as follows.

(1) Each vector of the basis in which the equal-time correlation matrix is written can be assigned to a certain time series $X_i(t)$ of the multivariate data set (channel basis).

(2) The increase of synchronization of K time series within an M-dimensional multivariate time series causes a repulsion of eigenstates of the correlation matrix, where K levels participate. This repulsion occurs between states at the edges of the spectrum. The number of increasing states at the upper edge and decreasing states at the lower edge is determined by the specific correlation structure of the data set.

(3) The eigenvectors involved in this repulsion process collect significant contributions of those components which belong to the correlated subspace. Hence, by investigating the structure of the eigenvectors it is possible to determine which of the time series are correlated. Additionally, the different types of correlations between subsystems (i.e., correlated, noncorrelated, anticorrelated dynamics) are directly reflected in the symmetry properties of the eigenvectors.

(4) There exist situations where the results extracted from the lower edge of the spectrum are more significant than the analysis of the largest states. Occasionally, as in the example given in Fig. 8(b), only the smallest eigenvalues (and eigenstates) deliver any significant information about changes of the correlation structure.

(5) The time-resolved estimation of the equal-time correlation matrix **C**, i.e., the shifting of a finite-length window Δt with a large overlap, provides dynamical information about which parts of the system are correlated at a certain time. The method extracts those subsystems which show collective behavior, and provides an ordering according to their degree of collectivity. Segments of the time series that are "interesting" in terms of increasing or decreasing collectivity of the dynamics of either the whole system or of transiently formed subsystems are detected automatically.

(6) In contrast to the case of, e.g., the Fourier transform, the finite size of the time window Δt does not present an approximation. While a Fourier transform performed over a finite sliding segment of the data always requires a compromise between a satisfactory time resolution and the desired spectral resolution, in the case of the equal-time correlation matrix Δt simply defines the time scale on which correlations are measured. Nevertheless, also in the case of the correlation matrix a compromise has to be made between the time scale given by Δt and the influence of noise and random correlations. Hence, the choice of the length of Δt strongly depends on the specific properties of the system under consideration, i.e., its typical time scales, the magnitude of noise contamination, and the sampling rate of the measurement.

The properties listed above have been demonstrated for different systems like N_f-tori, multivariate autoregressive processes, and coupled chaotic oscillators with a funnel attractor. By employing these systems we intended to define flexible testing systems for investigating whether phase correlations could be detected by analysis of the eigenvalues of correlation matrices. Furthermore, the situations simulated by the systems listed in Table I can be regarded as typical examples of principal correlation changes in spatially extended systems where multiple processes occur simultaneously, like for example human brain activity.

We believe that the techniques based on time resolved analysis of the equal-time correlation matrix provide promising tools for the detection and characterization of phase-shape correlations in multivariate data sets, independent of the particular system under consideration.

ACKNOWLEDGMENTS

M.M. thanks F. Leyvraz for fruitful discussions and the Institute of Statistical Mathematics (ISM), Tokyo, for kind hospitality. M.M. and G.B. thank M. López and Y. López for extensive discussions. This work was supported by CONACyT, Mexico (Project No. 40885-F). A.G. gratefully acknowledges support by the Deutsche Forschungsgemeinschaft (DFG) through Project No. GA 673/1-1 and by the Japanese Society for the Promotion of Science (JSPS).

[1] C. M. Gray, A. K. Engel, P. Koenig, and W. Singer, Nature (London) **338**, 334 (1989).
[2] R. Newbold Bracewell, *The Fourier Transform and Its Applications*, 3rd ed. (McGraw-Hill Science/Engineering/Math, New York, 1999).
[3] D. B. Percival and A. T. Walden, *Wavelet Methods for Time Series Analysis* (Cambridge University Press, Cambridge, U.K., 2000).
[4] M. Small, e-print nlin.CD/0320111.
[5] P. Grassberger and I. Procaccia, Physica D **9**, 189 (1983).
[6] A. S. Pikovsky, M. G. Rosenblum, and J. Kurths, *Synchronization* (Cambridge University Press, Cambridge, U.K., 2001).
[7] D. Gabor, J. Inst. Electr. Eng., Part 3 **93**, 429 (1946).
[8] S.-I. Amari and A. Cichocki, Proc.-IEEE Ultrason. Symp. **9**, 2026 (1998); J.-F. Cardoso, *ibid.* **9**, 2009 (1998).
[9] A. D. Back and A. S. Weigend, Int. J. Neural Syst. **8**, 473 (1998); R. Vigário, V. Jousmäki, M. Hämäläinen, R. Hari, and E. Oja, in *Advances in Neural Information Processing Systems* (MIT Press, Cambridge, MA, 1998), Vol. 10, p. 229.
[10] L. Laloux, P. Cizeau, J.-P. Bouchaud, and M. Potters, Phys. Rev. Lett. **83**, 1467 (1999).
[11] V. Plerou, P. Gopikrishnan, B. Rosenow, L. A. Nunes Amaral, and H. E. Stanley, Phys. Rev. Lett. **83**, 1471 (1999).
[12] V. Plerou *et al.*, Physica A **287**, 374 (2000).
[13] S. Drozdz, F. Gruemmer, F. Ruf, and J. Speth, Physica A **287**, 440 (2000); S. Drozdz, J. Kwapien, F. Gruemmer, F. Ruf, and J. Speth, *ibid.* **299**, 144 (2001); J. Kwapien, S. Drozdz, and J. Speth, *ibid.* **330**, 605 (2003).
[14] V. Plerou *et al.*, Phys. Rev. E **65**, 066126 (2002).
[15] S. Maslov, Physica A **301**, 397 (2001).
[16] J. Kwapien, S. Drozdz, and A. A. Ioannides, Phys. Rev. E **62**, 5557 (2000); J. Kwapien, S. Drozdz, L. C. Liu, and A. A. Ioannides, *ibid.* **58**, 6359 (1998).
[17] P. A. Tass *et al.*, Phys. Rev. Lett. **90**, 088101 (2003).
[18] M. S. Santhanam and P. K. Patra, Phys. Rev. E **64**, 016102 (2001).
[19] P. Seba, Phys. Rev. Lett. **91**, 198104 (2003).
[20] M. L. Mehta, *Random Matrices* (Academic Press, New York, 1990).
[21] R. J. Muirhead, *Aspects of Multivariate Statistical Theory* (John Wiley & Sons, New York, 1982).
[22] I. T. Jolliffe, *Principal Component Analysis* (Springer-Verlag, Berlin, 1986); M. Kendall, *Multivariate Analysis* (Charles Griffin & Co., London, 1975).
[23] A. Bohr and B. R. Mottelson, *Nuclear Structure* (Benjamin, New York, 1969), Vols. 1 and 2.
[24] M. Müller, F.-M. Dittes, W. Iskra, and I. Rotter, Phys. Rev. E **52**, 5961 (1995).
[25] C. Jung, M. Müller, and I. Rotter, Phys. Rev. E **60**, 114 (1999).
[26] E. Persson and I. Rotter, Phys. Rev. C **59**, 164 (1999).
[27] A. Galka and G. Pfister, Int. J. Bifurcation Chaos Appl. Sci. Eng., **13**, 723 (2003).
[28] J. D. Noh, Phys. Rev. E **61**, 5981 (2000).
[29] V. M. Eguiluz and M. G. Zimmermann, Phys. Rev. Lett. **85**, 5659 (2000); R. D'Hulst and G. J. Rodgers, e-print cond-mat/9908481; D. Zheng, G. J. Rodgers, P. M. Hui, and R. D'Hulst, e-print cond-mat/0108399.
[30] G. E. P. Box and G. M. Jenkins, *Time Series Analysis, Forecasting and Control* (Holden-Day, San Francisco, 1970).
[31] M. G. Rosenblum *et al.*, Phys. Rev. Lett. **89**, 264102 (2002).
[32] A. Hyvärinen and E. Oja, Neural Comput. **9**, 1483 (1997); A. Hyvärinen, IEEE Trans. Neural Netw. **10**, 626 (1999); A. Hyvärinen, Neural Process. Lett. **11**, 1739 (1999).
[33] E. Niedermeyer, in *Electroencephalography*, edited by E. Niedermeyer and F. Lopes da Silva, 4th ed. (Lippincott Williams & Wilkins, Philadelphia, 1999).
[34] R. Friedrich, in *Chaos in Brain?*, edited by K. Lehnertz, J. Arnold, P. Grassberger, and C. E. Elger (World Scientific, Singapore, 1999), p. 156.
[35] E. P. Wigner, Ann. Math. **53**, 36 (1951).
[36] E. P. Wigner, Proc. Cambridge Philos. Soc. **47**, 790 (1951).
[37] F. J. Dyson, J. Math. Phys. **3**, 140 (1962); F. J. Dyson and M. L. Mehta, *ibid.* **4**, 701 (1963); M. L. Mehta and F. J. Dyson, *ibid.* **4**, 713 (1963).
[38] T. A. Brody *et al.*, Rev. Mod. Phys. **53**, 385 (1981).
[39] T. Guhr, A. Müller-Groeling, and H. A. Weidenmüller, Phys. Rep. **29**, 190 (1998).
[40] F. Haake, *Quantum Signatures of Chaos*, 2nd ed., Springer Series in Synergetics Vol. 54 (Springer, Berlin, 2001).
[41] J. Flores, M. Horoi, M. Müller, and T. H. Seligman, Phys. Rev. E **63**, 026204 (2000).
[42] A. M. Sengupta and P. P. Mitra, Phys. Rev. E **60**, 3389 (1999).
[43] M. J. Bowick and E. Brézin, Phys. Lett. B **268**, 21 (1991); J. Feinberg and A. Zee, J. Stat. Phys. **87**, 473 (1997).
[44] Y. Malevergne and D. Sornette, Physica A **331**, 660 (2004).